EFFICIENCY IMPROVEMENT IN TiO_2-PARTICLE BASED SOLAR CELLS AFTER DEPOSITION OF METAL IN SPACES BETWEEN PARTICLES

Sahrul Saehana, Rita Prasetyowati, Marina I. Hidayat, Pepen Arifin, Khairurrijal, and Mikrajuddin Abdullah[(a)]

Physics of Electronics Materials Research Division,Faculty of Mathematics and Natural Sciences Bandung Institute of Technology

[a]e-mail address: din@fi.itb.ac.id

We report the fabrication of solar cells employing TiO_2 particles as the active light-absorbing material. The solar cells were prepared by depositing TiO_2 particles on a transparent conducting electrode (ITO), followed by a polymer electrolyte and a counter electrode. Copper particles were deposited in the spaces between the particles prior to deposition of the polymer electrolyte, forming continuous copper bridges to quickly transport generated photoelectrons from the particle surfaces to the transparent electrode, reducing electron/hole recombination. Several metal deposition methods were used including sputtering, electroplating, and doctor-blade coating. This strategy resulted in significant enhancement of the solar conversion efficiency compared to a similar design constructed without the copper coating.

Keywords: metal-semiconductor junction, performance and solar cells.

INTRODUCTION

TiO_2 is widely used in solar energy applications such as photovoltaic cells (Grätzel, 2003; Ribiero, et al., 2009; Wang et al., 2009; Tachibana et al., 2008; Singh et al., 2009), air and water purification (Birnie et al., 2006; Kabra et al., 2009; Hashimoto et al., 2005) and UV absorption in cosmetics (Jaroenworaluck et al., 2006). It has been employed in dye sensitized solar cells (DSSC) and bulk heterojunction solar cells (BHJ) to obtain high conversion efficiencies (Chiba et al., 2006) coupled with easy fabrication (Huang et al., 2007), low cost (O'Regan et al., 1991; Joshi et al., 2009), low toxicity (Sommeling et al., 2004), and long-term stability (HaiLing et al., 2009). However, the rapid rate of electron-hole recombination on TiO_2 particles (Figure 1) makes the efficiency of TiO_2-based solar cells without dyes quite low.

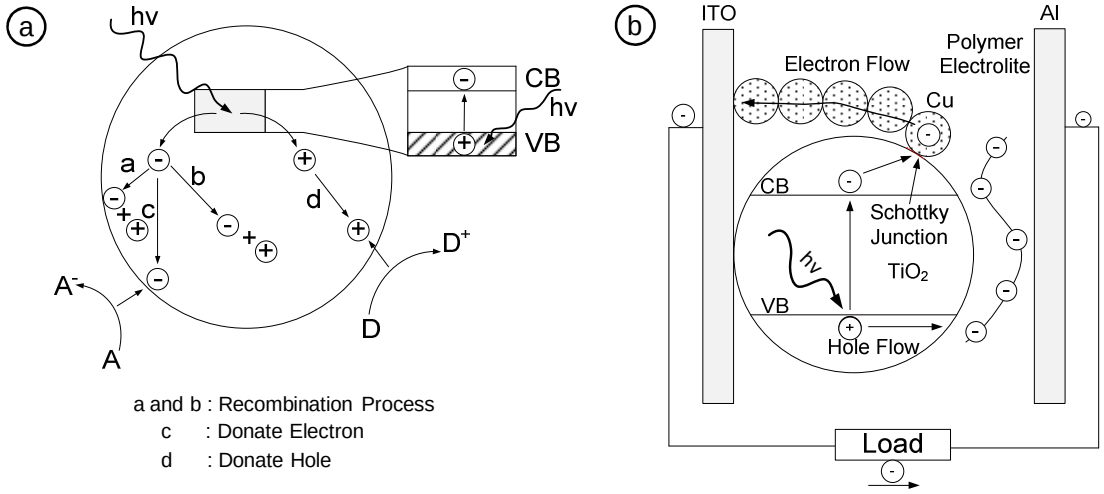

Figure 1 (a) Photoexcitation process on TiO_2 surface and (b) Design of solar cells.

Several recent reports have described efficiency enhancements in TiO_2 solar cells. A popular method is to minimize electron-hole recombination by depositing metal on the semiconductor surface (Pan et al., 2007; Cai et al., 2008; Subramanian et al., 2004; Behnajady et al., 2008; Chen et al., 2007; Subramanian et al., 2001; Gnaser et al., 2004; Diebolt, 2003; Wang et al., 2008; Hajkova et al., 2009; Grabowska et al., 2010; Linsebigler et al., 1995). The excited electrons are trapped at the metal surface, increasing charge carrier lifetimes.

In order to decrease recombination of electron-hole pairs and increase quantum efficiency of the photocatalytic process, we modified TiO_2 thin films using an interconnected metal (Cu) for electron transport (Figure 1b) (Sommeling et al., 2004; Fuke et al., 2007). The cells employed a polymer electrolyte composed of polyethylene glycol and a lithium salt for hole transport and to increase the short circuit current (Wang et al., 2008; Wu et al., 2008; Jiang et al., 2003; Kang et al., 2005). The copper was deposited using sputtering, doctor-blade coating, or electroplating. We also investigated the effect of metal particle size on cell performance. A subsidiary goal of the study was to demonstrate the use of simple and low-cost methods such as electroplating for depositing metal on TiO_2 surfaces.

EXPERIMENTAL

Materials

TiO_2 was purchased from Bratachem, Indonesia. Cu_2SO_4, copper powder, lithium hydroxide monohydrate (LiOH), and polyethylene glycol (PEG, n=20,000) were purchased from Merck, Indonesia. ITO with a sheet resistance of 100 Ω/cm^2 was purchased from Solaronix, Switzerland.

Preparation of copper-coated TiO_2 nanoparticles

Sputtering methods

The deposition parameters for fabrication of Cu/TiO_2 structures are summarized in Table 1.

Table 1 Deposition parameters for Cu/TiO_2 structures.

Parameter	Value
Flow rate of Ar, sccm	100
Heater temperature, °C	150
Pressure, Bar	0.71
Time deposition, sec	300
I_{Plasma}, mA	39
V_{Plasma}, V	600

Electroplating methods

Copper coatings were prepared using a Watts-type bath containing 20 mL copper sulfate (Cu_2SO_4). A copper rod of 99.99% purity with dimensions of 5 cm was used as the anode and the TiO_2 film deposited on an ITO-coated glass substrate was used as the cathode. The electroplating conditions are listed in Table 2.

Table 2 Electroplating conditions for Cu coating.

Parameter	Value
Current, A	1.0
Voltage, V	5.0
Deposition time, s	10.0
Solution concentration, M	0.1
Volume of solution, mL	20.0
Distance anode-cathode, cm	5.0
ITO resistance, Ω/cm^2	100
Bath temperature, °C	25

Doctor-blade methods

Nanocomposites were prepared by dissolving 0.7 g PEG in 10 mL of water at 80°C for 2 hours, then adding 1 g TiO_2 and 0.1 g Cu and stirring until gelation occurred. The Cu/TiO_2 nanocomposites were deposited on an ITO-coated glass substrate by applying the doctor-blade technique. The films were heated on a hot plate at 80^oC for 5 min. The process is illustrated in Figure 2.

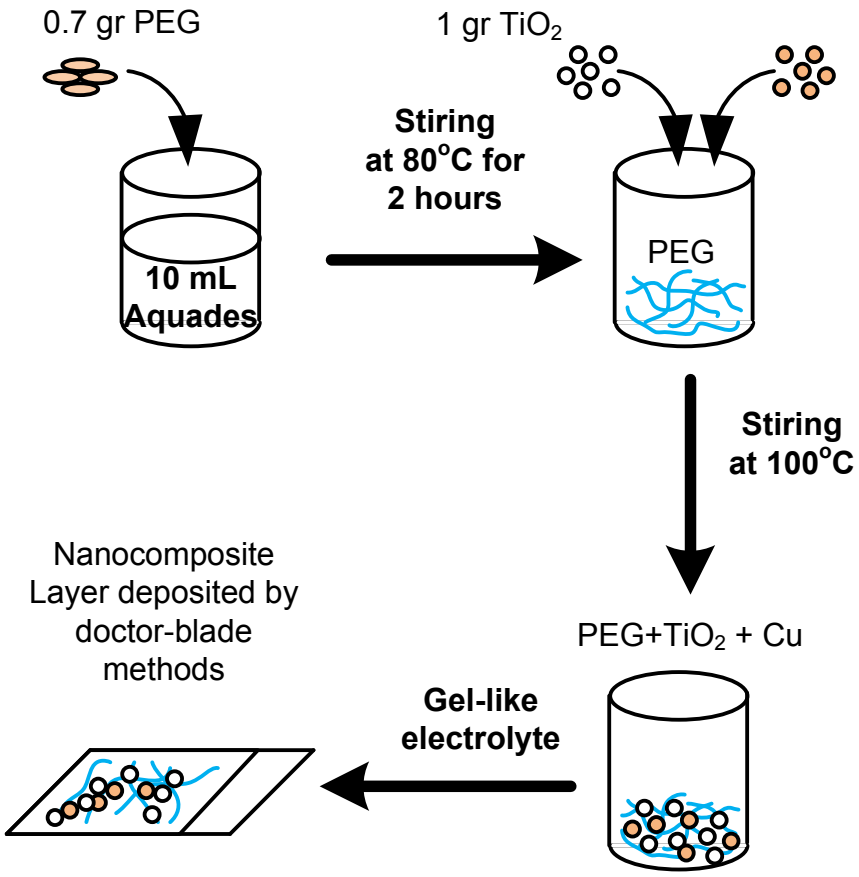

Figure 2 Doctor-blade coating process for producing Cu/TiO_2 nanocomposite films.

Characterization of TiO_2 films

The optical absorbance of the films was determined using a Cary 100 UV/Vis spectrometer. The surface morphology and film composition were examined using a JEOL JSM-6360LA SEM equipped with an EDX attachment. The structure of the films was investigated using XRD on a PW1710 diffractometer.

Procedures

The solar cells consisted of an ITO electrode, a TiO_2 layer coated with metal (Cu), a gel polymer electrolyte layer, and an Al counter electrode.

The ITO-coated glass substrate (1 cm^2) was sonicated in water for 15 min, followed by 70% alcohol for 30 min. A suspension was prepared by dispersing 10 g TiO_2 in 10 mL of water and mixing with a magnetic stirrer for 45 min. The TiO_2 suspension was sprayed on the substrate at a temperature of 150 °C (Halme et al., 2006). The spray process was repeated 30 times. The resulting thick film of TiO_2 was heated on a hot plate at 250 °C for 30 min to evaporate water, then sintered at 450 °C for 30 min to improve the electrical contact between the TiO_2 particles and the ITO. The films were then coated with Cu.

The polymer electrolyte was made by dissolving 0.5 g LiOH (Bratachem, Indonesia) in 10 mL water and adding 0.8 g polyethylene glycol (PEG, Merck). The mixture was heated with stirring at

110 °C for 1 hour to produce a gel-like electrolyte. The electrolyte was manually applied to the Cu/TiO_2 layer and an aluminum counter electrode was added.

RESULTS AND DISCUSSION

Characterization of TiO_2 and Cu-coated TiO_2 films

The UV-Vis spectrum of a TiO_2 electrode is presented in Figure 3(a). The electrode absorbs over a very broad range, from less than 200 nm to more than 800 nm, in contrast to the pure TiO_2 spectrum of Figure 3(b). The broad absorption spectrum suggests these devices are potentially excellent solar harvesting devices.

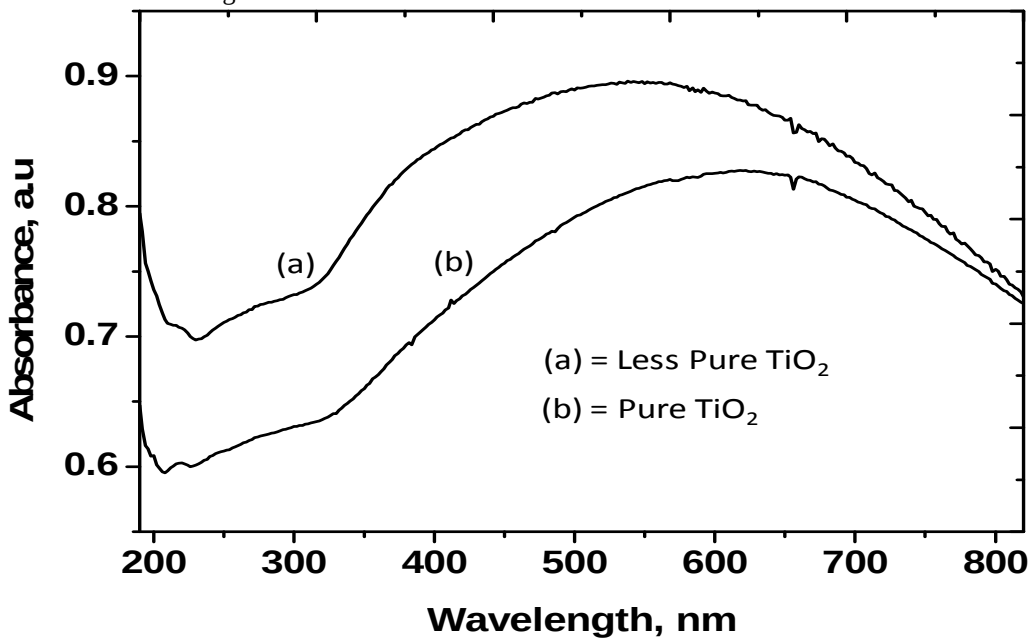

Figure 3 Absorption spectra of modified (a) and pure (b) TiO_2 films.

The morphology of TiO_2 was determined using electron dispersive X-ray analysis and SEM. The particles are sub-micrometer in size, with a minimum value of approximately 192 nm. Figure 4(a) is a micrograph of the TiO_2 electrode. The film surface is smooth and uniform with equally distributed nanometer sized grains. According to the theory of Usami and Ozaki the grains could also improve conversion efficiency through multiple scattering events (Bi-Tao et al., 2008).

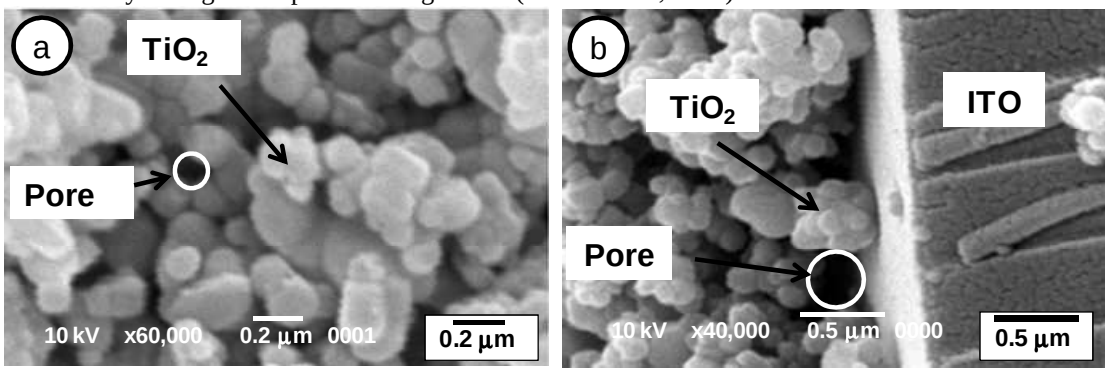

Figure 4 SEM images of TiO_2 film without Cu nanoparticles: (a) surface and (b) cross section.

The porous TiO_2 electrode formed using the spray method provides pore sizes of 50-300 nm and a thickness of 5-6 µm. Figure 4(b) is a cross-sectional view of the film. It is expected that during electroplating nucleation of Cu nanoparticles begins in the pores of TiO_2. Inside the film there is not much difference in grain size between TiO_2 and Cu.

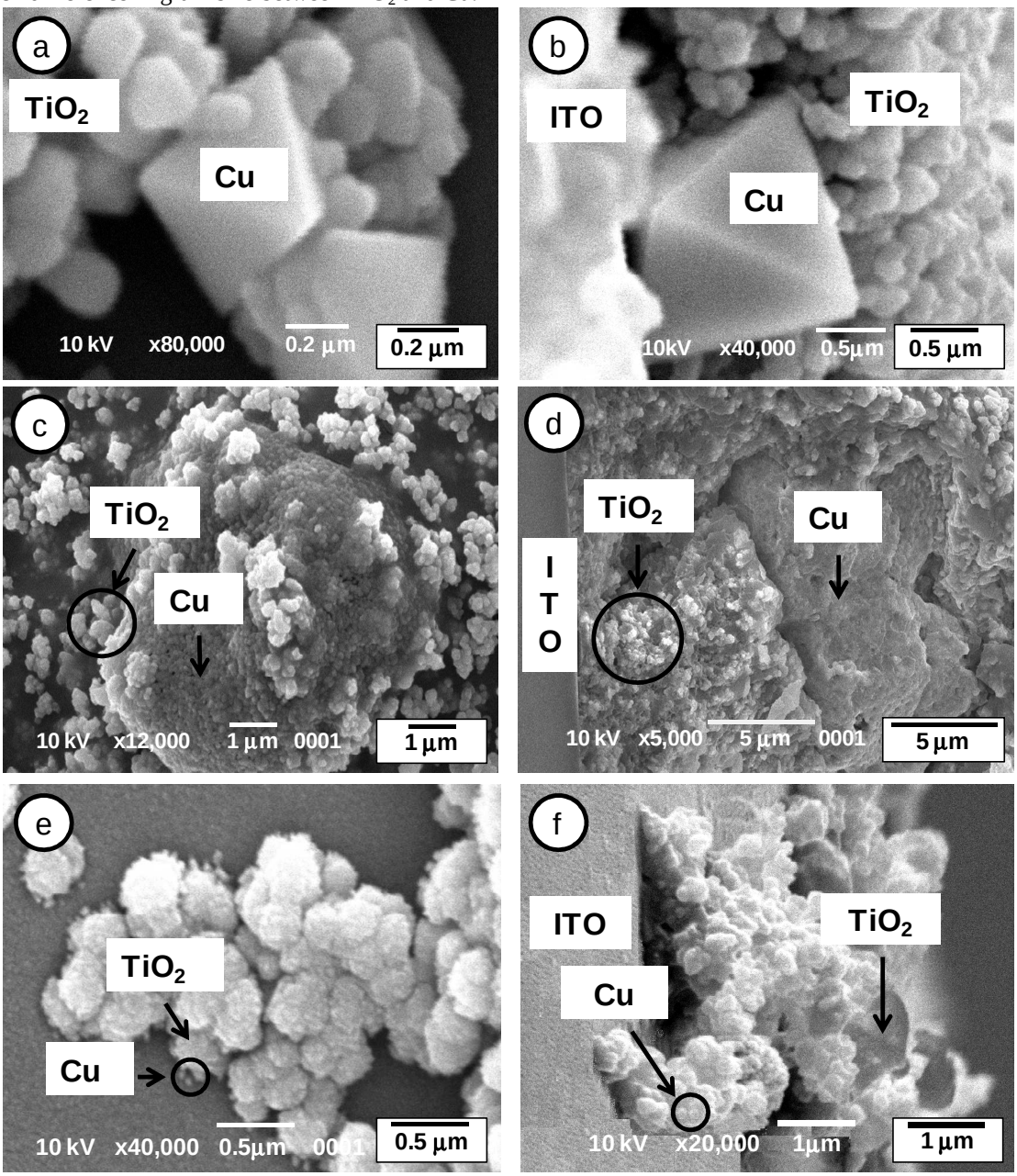

Figure 5 Surface and cross-section of Cu/TiO_2 films after coating using: electroplating methods (a,b), doctor-blade (c,d), and sputtering (e,f).

Figures 5(a) and (b) illustrate the Cu films grown in the pores and on the surface of the TiO_2 film using electroplating. The diamond-shaped Cu grains are larger than the TiO_2 particles and make

contact with each other. It is assumed that the excited electrons generated in the TiO_2 are trapped in the Cu particles. Figures 5(c) and (d) are images of the Cu/TiO_2 nanocomposite film formed using the doctor-blade method. The bulk Cu is in contact with the TiO_2 particles. Conversely, SEM images of Cu/TiO_2 structures prepared using sputtering (Figures 5(e) and (f)) reveal that the Cu distribution is not uniform and that the deposit consists of isolated small grains of Cu in contact with TiO_2 particles.

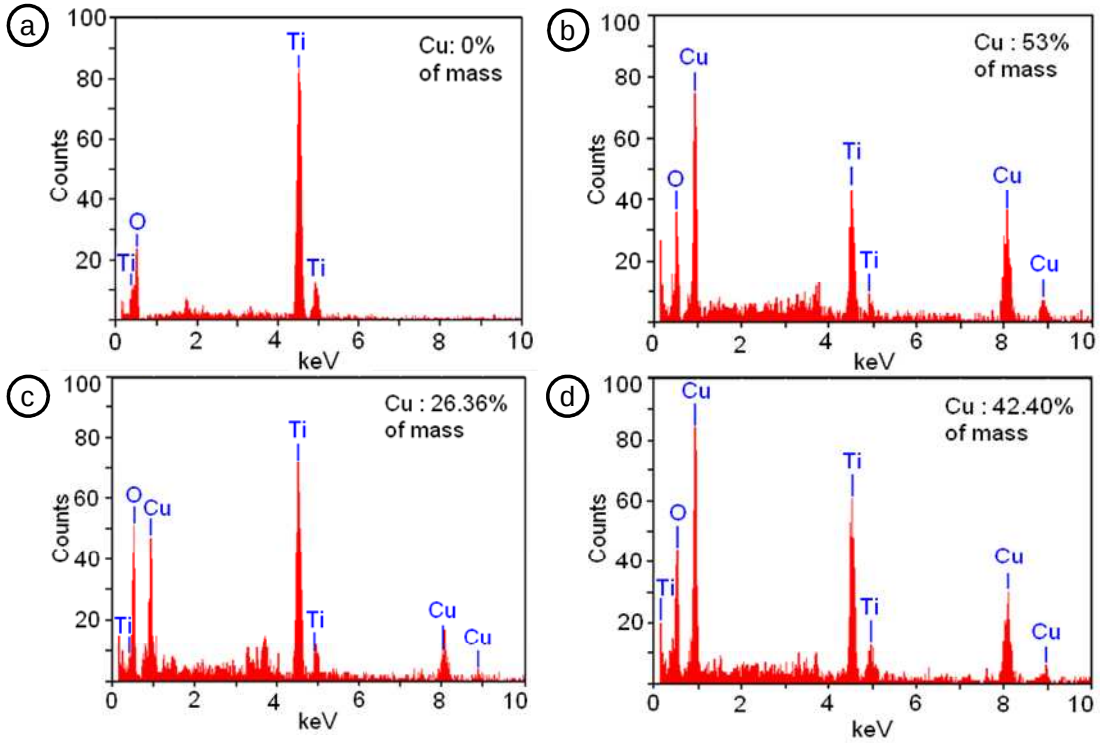

Figure 6 Elemental analysis of TiO_2 films: (a) Uncoated TiO_2, (b) Cu/TiO_2 (doctor-blade), (c) Cu/TiO_2 (sputtering), and (d) Cu/TiO_2 (electroplating)

Elemental analyses of TiO_2 films based on EDX analysis were also performed using the JEOL JSM-6360LA. Figure 6 contains the EDX spectra of uncoated and coated TiO_2. The peaks in figure 6(a) correspond to Ti and O, demonstrating that the film is essentially pure. Figures 6(b), (c), and (d) display Cu peaks, indicating that the TiO_2 films were successfully coated with Cu to the extent of 53.27%, 26,36%, or 40.86%.

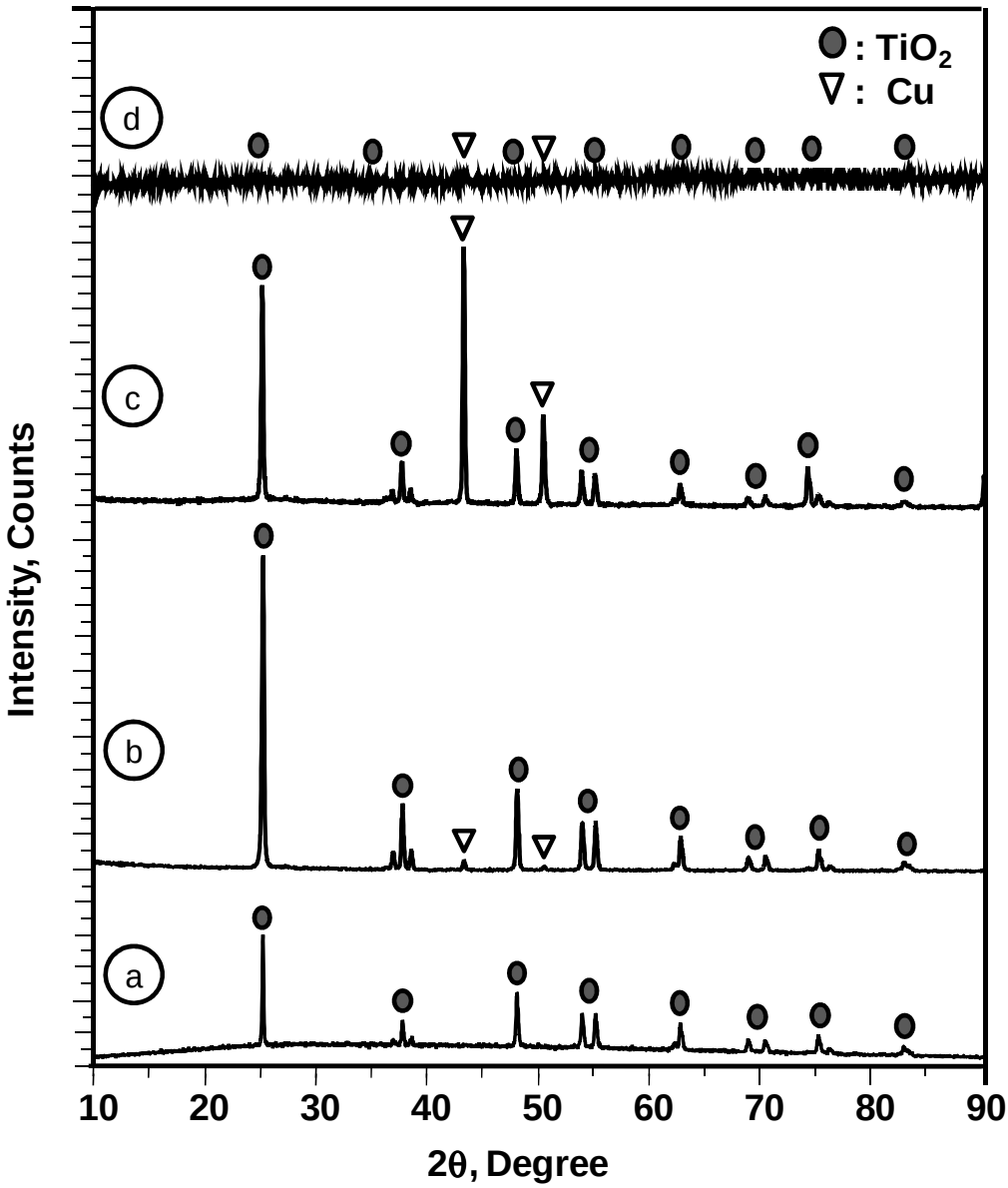

Figure 7 X-ray diffraction pattern of: (a) Uncoated TiO_2, (b) Cu/TiO_2 (electroplating), (c) Cu/TiO_2 (doctor-blade), and (d) Cu/TiO_2 (sputtering).

The XRD patterns of pure and Cu-coated TiO2 nanoparticles appear in Figure 7, for 2θ diffraction angles between 10° and 90°. The XRD pattern of TiO2 exhibits primary peaks at 25°, 38°, 49°, and 83°, which may be attributed to the diffraction planes of anatase TiO2. The two peaks at 40° and 52° may be attributed to the diffraction planes of Cu.

The average size (D) of the Cu particles was determined from the XRD patterns of several Cu/TiO2 samples (Figure 7) using Scherer's equation (Table 3).

$$D = \frac{k\,\lambda}{\beta\ \mathrm{Cos}\,\theta} \qquad (1)$$

In this equation, k is a constant equal to 0.9, λ is the x-ray wavelength (equal to 0.154 nm), β is the full width of the peak at half-maximum, and θ is half of the diffraction angle (Abdullah et al., 2010).

Effect of Cu coating on cell performance

The performance of the devices was measured using a current-voltage (I-V) meter (Keithley 617). The measurements were obtained in the dark and under xenon lamp illumination. Light intensity was measured using a luxmeter (Lutron LX-101). The results depicted in figure 8 indicate that the interlayer electrical connections are well-developed.

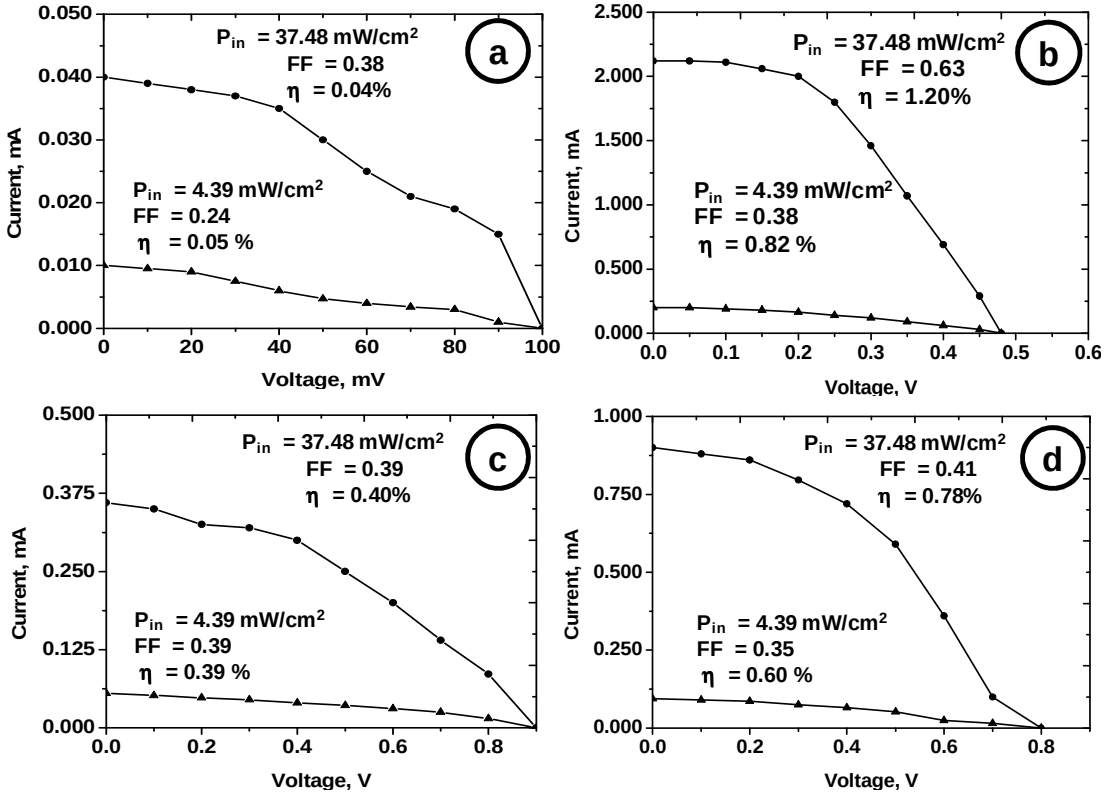

Figure 8 Photocurrent and voltage characteristics of: (a) Uncoated TiO_2, (b) Cu/TiO_2 (sputtered), (c) Cu/TiO_2 (doctor-blade), and (d) Cu/TiO_2 (electroplated).

The performance was characterized under AM 1.5 illumination at high (37.48 mW/cm2) and low (4.39 mW/cm2) intensities. The efficiency η under xenon illumination was calculated using $\eta = (V_{oc} I_{sc} FF / P_{in}) \times 100\%$, in which Voc is the open-circuit voltage, Isc is the short-circuit current, FF is the fill factor, and Pin is the total radiant power received by the cell.

The efficiencies of the solar cells described here were greater than the results of our previous study (Abdullah et al., 2010; Saehana et al., 2010), but the FF was still very low. Under intense irradiation, the efficiencies were approximately 1.20%, 0.40%, and 0.78%. Under lower intensity illumination, the efficiencies were 0.82%, 0.39%, and 0.60%. The poor performance may be due to the poor fill factor, short-circuit current, or open-circuit voltage, which in turn may be affected by the high sheet resistance of TiO2 films (Ahn et al., 2007; Han et al., 2006).

The results illustrated in figure 8 clearly indicate that the performance of Cu/TiO2 film devices is greater than devices employing uncoated TiO2 films. This is caused by the high Schottky

barrier of metals deposited on the TiO2 that enables them to act as electron traps, facilitating electron capture. According to Hailing (2009), electron capture by metals increases electron-hole pair separation lifetime by hindering the recombination of electron-hole pairs and promoting interfacial electron transfer processes.

Figure 9(a) is a schematic diagram depicting an electron trapped at the Schottky barrier of a metal/semiconductor interface, highlighting the small area of the semiconductor surface actually covered by the metal. In scheme 9(a), the excited electron moves to the metal and becomes trapped, reducing electron-hole recombination. The migration of electrons to the metal particles was confirmed by studies indicating a reduction in the photoconductance of the semiconductor in Cu/TiO2 devices compared to those using TiO2 alone (Linsebigler et al., 1995). Figure 9(b) contains the band diagram of a metal and semiconductor in contact at equilibrium, in which electrons flow to the metal from the semiconductor.

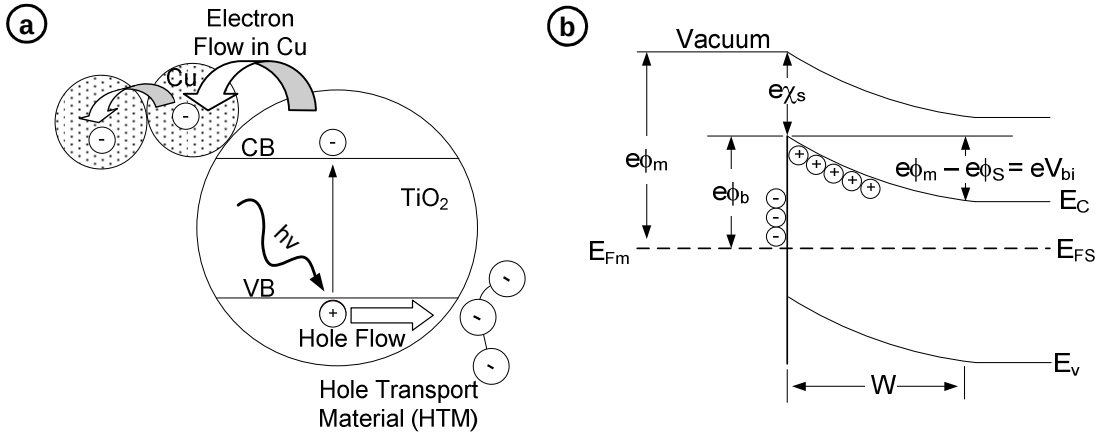

Figure 9 (a) Mechanism of photoexcitation process in Cu-deposited TiO_2 under UV irradiation, and (b) band diagram of metal-semiconductor (Schottky) junction at equilibrium.

Electronic modification of the semiconductor surface via metal deposition has been observed with other noble metals such as Pt, Ag, and Au. The addition of metal to the TiO2 surface may cause trapping of electrons at the metal sites (Diebolt, 2003; Duncan et al., 2007).

The results plotted in Figure 10 also demonstrate that the performance of Cu/TiO2 sputtered films was higher devices produced using electroplating or doctor-blade methods. The difference in performance may be caused by the particle size and distribution of copper on the TiO2 film.

Effect of Copper Size and Content on Performance of Solar Cell

The performance of the Cu/TiO2 composite system was initially enhanced with increasing Cu content (HaiLing et al., 2009), but decreased after reaching a critical Cu loading value due to bulk effects. Copper has a high work function and displays a stronger bulk effect than materials such as Au, Ag, and Pt. Large metal particle sizes decreased the performance of the cells.

The electron affinity of copper is 119.24 kJ/mol and the work function is 4.65 eV. The ability of a metal to accept an electron from a semiconductor is related to the electron affinity, with higher affinity metals more easily accepting electrons. Conversely, the work function describes the facility of electron migration from the interior to the surface of a metal, with smaller values indicating easier migration. A synergistic tradeoff between these two values determines the performance of this type of solar cell. However copper is a relatively cheap metal, and surface modification with Cu still improves TiO2 thin-film performance.

Table 3 Comparison between Cu/TiO_2 solar cells fabricated using sputtering, electroplating, and doctor-blade methods.

Copper Deposition Method	Mass Content of Cu, %	Grain Size of Cu, nm	Efficiency of Solar Cells, %
Sputtering	26.36	78.42	1.20
Electroplating	42.40	228.75	0.78
Doctor-Blade	53.27	1,863	0.40

Cu/TiO2 solar cells coated using sputtering displayed higher efficiencies than other methods. This may be an effect of grain size (Rashidi et al., 2010), the high doping content (Subramanian et al., 2004), or the large fraction of metal deposited on the surface causing electron accumulation on the particles and lower quantum efficiency. However, the electroplating method has potential for further development and improvement through parameter optimization.

Effect of Polymer Electrolyte on Performance

We also investigated the use of a polymer electrolyte containing Li+ to improve the device stability and prevent solvent evaporation. The use of a gel polymer electrolyte with a conductivity of 0.16 S/cm also increased the speed of electron migration in TiO2 and enhanced the short-circuit current and open-circuit voltage of the solar cells (Wu et al., 2008; Aravindan et al., 2007). According to Wang et al. (2008), Li+ ion creates new trapping states that contribute to electron injection into the TiO2 conduction band. Increases in electrolyte conductivity increase the short-circuit current. However, in this study conductivity optimization was not performed.

CONCLUSION

Copper coated TiO2 films were more efficient than uncoated TiO2 films in terms of photovoltaic activity. This may be the result of a well-developed metal-semiconductor junction (Schottky junction) hindering electron-hole recombination. Considering metal bulk effects, we also found that the efficiency of solar cells prepared using a sputtering method was higher than those constructed using electroplating or doctor-blade methods, possibly because of grain size or copper content.

ACKNOWLEDGEMENTS

This work was supported by research grants from Asahi Glass Foundation 2010, Hibah Strategis Nasional DIPA-ITB (Bandung Institute of Technology) 2010, and Hibah Doktor 2010.

REFERENCES

1. Abdullah, M., Nurmawarti, I., Subianto, H., Khairurrijal, Mahfudz, H. (2010). Very wide band absorption of sunlight spectra using titanium dioxide particles with distributed band gap. Jurnal Nanosains & Nanoteknologi 3: 10-14.
2. Abdullah, M., Khairurrijal. (2010). Karakterisasi Nanomaterial: Teori, Penerapan dan Pengolahan Data. Bandung: Rezeki Putra Bandung Press.
3. Ahn, J.H., Mane, R.S., Todkar, V.V., Han, S.H. (2007). Invasion of CdSe nanoparticles for photosensitization of porous TiO2. International Journal of Electrochemical Science 2: 517-522.
4. Aravindan, V., Vickraman, P. (2007). Effects of TiO2 and ZrO2 nanofillers in LiBOB based PVdF/PVC composite polymer electrolytes (CPE). Journal of Physics D: Applied Physics 42: 6754.
5. Behnajady, M.A., Modirshahla, N., Shokri, M., Rad, B. (2008). Enhancement of photocatalytic activity of TiO2 nanoparticles by silver doping: photodeposition versus liquid impregnation methods. Global NEST Journal 10: 1-7.
6. Bi-Tao, X., Bao-Xue, Z., Jing, B., Qing, Z., Yan-Biao, L., Wei-Min, C., Jun, C. (2008). Light scattering of nanocrystalline TiO2 film used in dye-sensitized solar cells. Chinese Physics B 17: 3714-3719.
7. Birnie, M., Gillott, M., Riffat, S. (2006). The immobilization of titanium dioxide on organic polymers, for a cost effective and energy efficient means of improving indoorair quality. International Journal of Green Energy 3: 101–114.
8. Cai, C., Zhang, J., Pan, F., Zhang, W., Zhu, H., Wang, T. (2008). Influence of metal (Au, Ag) micro-grid on the photocatalytic activity of TiO2 film. Catalysis Letter 123: 51-55.
9. Chen, H.W., Ku, Y., Kuo, Y. L. (2007). Effect of Pt/TiO2 characteristics on temporal behavior of o-cresol decomposition by visible light-induced photocatalysis. Water Research 41: 2069-2078.
10. Chiba, Y., Islam, A., Watanabe, Y., Komiya, R., Koide, N., Han, L. (2006). Dye-sensitized solar cells with conversion e□ciency of 11.1%. Japanese Journal of Applied Physics 45: L638-L640.
11. Diebolt, U. (2003). The surface science of titanium dioxide. Surface Science Reports 48: 53-229.
12. Duncan, W.R., Prezhdo, O.V. (2007). Theoretical studies of photoinduced electron transfer in dye-sensitized TiO2. Annual Review of Physical Chemistry 58: 143–84.
13. Fuke, N., Fukui, A., Chiba, Y., Komiya, R., Yamanaka, R., Han, L. (2007). Back contact dye-sensitized solar cells. Japanese Journal of Applied Physics 46: L420–L422.
14. Gnaser, H., Huber, B., Ziegler, C. (2004). Nanocrystalline TiO2 for photocatalysis. Encyclopedia of Nanoscience and Nanotechnology 6: 505–535.
15. Grabowska, E., Remita, H., Zaleksa, A. (2010). Photocatalytic activity of TiO2 loaded with metal clusters. Physicochemical Problem of Minerals Processing 45: 29-38.
16. Grätzel, M. (2003). Review: Dye-sensitized solar cells. Journal of Photochemical and Photobiology.: Photochemical Reviews 4: 145–153.
17. HaiLing, Z., JunYing, Z., TianMin, W., LiuGang, W., Xiang, L., BaiBiao, H. (2009). Photocatalytic performance of TiO2 thin films connected with Cu micro-grid. Science in China Series E: Technological Science 52: 2175-2179.
18. Hajkova, P., Spatenka, P., Krumeich, J., Exnar, P., Kolouch, A., Matousek, J. (2009). The influence of surface treatment on photocatalytic activity of PECVD TiO2 thin films. Plasma Processes and Polymers 6: 735–740.
19. Halme, J., Saarinen, J., Lund, P. (2006). Spray deposition and compression of TiO2 nanoparticle films for dye-sensitized solar cells on plastic substrates. Solar Energy Materials & Solar Cells 90: 887–899.

20. Han, L., Koide, N., Chiba, Y., Islam, A., Mitate, T. (2006). Modeling of an equivalent circuit for dye-sensitized solar cells: improvement of efficiency of dye-sensitized solar cells by reducing internal resistance. Comptes Rendus Chimie 9: 645–651.
21. Hashimoto, K., Irie, H., Fujishima, A., (2005). TiO2 photocatalysis: a historical overview and future prospects. Japanese Journal of Applied Physics 44: 8269–8285.
22. Huang, Z., Liu, X., Li, K., Li, D., Luo, Y., Li, H., Song, W., Chen, L.Q., Meng Q. (2007). Application of carbon materials as counter electrodes of dye-sensitized solar cells. Electrochemistry Communication 9: 596-598.
23. Jaroenworaluck, A., Sunsaneeyametha, W., Kosachan, N., Stevens, R. (2006). Characteristics of silica-coated TiO2 and its UV absorption for sunscreen cosmetic applications. Surface and Interface Analysis 38: 473-477.
24. Jiang K J, Sun Y L, Shao K F, Wang J F and Yang L M (2003). Dye-sensitized TiO2 solid solar cell using poly (4-vinylphenyloxy-methyltriphenylamine) as hole transport material. Chinese Chemical Letters 14: 1093-1096.
25. Joshi, P., Xie, Y., Ropp, M., Galipeau, D., Bailey, S., Qiao, Q. (2009). Dye-sensitized solar cells based on low cost nanoscale carbon/TiO2 composite counter electrode. Energy & Environment Science 2: 333–440.
26. Kang, M.S., Kim, J.H., Kim, Y.J., Won J., Park, N.G., Kang, Y.S. (2005). Dye-sensitized solar cells based on composite solid polymer electrolytes. Chemical Communications, 889–891.
27. Kabra, K., Chaudhary, R., Sawhney, R.L. (2009). Application of solar photocatalytic treatment to industrial wastewater from a chrome plating unit. International Journal Of Green Energy 6: 83-91.
28. Linsebigler, A.L., Lu, G., Yates, J.T. (1995). Photocatalysis on TiO2 surfaces: principles, mechanisms, and selected results. Chemical Reviews 95: 735-758.
29. O'Regan, B., Grätzel, M. (1991). A low-cost, high-efficiency solar cells based on dye-sensitized colloidal TiO2 film. Nature 353: 737-740.
30. Pan, F., Zhang, J., Zhang, W., Wang, T., Cai, C. (2007). Enhanced photocatalytic activity of Ag microgrid connected TiO2 nanocrystalline films. Applied Physics Letters 90: 122114.
31. Rashidi, A.M., Amadeh, A. (2010). Effect of electroplating parameters on microstructure of nanocrystalline nickel coatings. Journal of Materials Science & Technology 26: 82-86.
32. Ribeiro, H.A., Sommeling, P.M., Kroon, J.M., Mendes, A., Costa, C.A.V. (2009). Dye-sensitized solar cells: novel concepts, materials, and state-of-the-art performances. International Journal of Green Energy 6: 245–256.
33. Saehana, S., Prasetyowati, R., Hidayat, M.I., Abdullah, M., Khairurrijal. (2010). Nanocomposite solar cells from “dirty” TiO2 nanoparticles. The Proceeding of 3rd Nanoscience and Nanotechnology Symposium : 154-157.
34. Singh, P.K., Kim, K.W., Nagarale, R.K., Rhee H.W. (2009). Preparation, characterization and application of ionic liquid doped solid polymer electrolyte membranes. Journal of Physics D: Applied Physics 42: 125101-125104.
35. Sommeling, P. M., Späth M., Smit, H.J.P., Bakker, N.J. Kroon, J.M. (2004). Long-term stability testing of dye-sensitized solar cells. Journal of Photochemistry and Photobiology A: Chemistry 164: 137–144.
36. Subramanian V., Wolf E.E., Kamat, P.V. (2004). Catalysis with TiO2/gold nanocomposites effect of metal particle size on the fermi level equilibration. Journal of American Chemical Society 126: 4943-4950.
37. Subramanian, V., Wolf, E.E. and Kamat, P.V. (2001). Semiconductor-metal composite nanostructures. To what extent do metal nanoparticles improve the photocatalytic activity of TiO2 films?. The Journal of Physical Chemistry B 105: 11439-11446.
38. Tachibana, Y., Umekita, K., Otsuka, Y., Kuwabata, S. (2008). Performance improvement of CdS quantum dots sensitized TiO2 solar cells by introducing a dense TiO2 blocking layer. Journal of Physics D: Applied Physics 41: 102002-102007.

39. Wang, M., Huang, C., Cao, Y., Yu, Q., Deng, Z., Liu Y., Huang, Z., Huang, J., Huang, Q., Guo, W., Liang, J. (2009). Dye-sensitized solar cells based on nanoparticle-decorated ZnO/TiO2 core/shell nanorod arrays. Journal of Physics D: Applied Physics 42: 155104-155110.
40. Wang, Q., Zhang, Z., Zakeeruddin, S.M., Grätzel, M. (2008). Enhancement of the performance of dye-sensitized solar cell by formation of shallow transport levels under visible light illumination. The Journal of Physical Chemistry C 112: 7084-7092.
41. Wang, X., Mitchell, D.R.G., Prince, K., Atanacio, A.J., Caruso, R.A. (2008). Gold nanoparticle incorporation into porous titania networks using an agarose gel templating technique for photocatalytic applications. Chemical of Material 20: 3917–3926.
42. Wu, J., Lan, Z., Hao, S., Li, P., Lin, J., Huang, M., Fang, L., Huang, Y. (2008). Progress on the electrolytes for dye-sensitized solar cells. Pure and Applied Chemistry 80: 2241–2258.